Published online 26 September 2016

Nucleic Acids Research, 2017, Vol. 45, No. 2 ***619–630***
doi: 10.1093/nar/gkw855

Crosstalk between androgen and pro-inflammatory signaling remodels androgen receptor and NF-κB cistrome to reprogram the prostate cancer cell transcriptome

Marjo Malinen[1,†], Einari A. Niskanen[1,†], Minna U. Kaikkonen[2] and Jorma J. Palvimo[1,*]

[1]Institute of Biomedicine, University of Eastern Finland, 70211 Kuopio, Finland and [2]A.I. Virtanen Institute, University of Eastern Finland, 70211 Kuopio, Finland

Received July 9, 2016; Revised September 14, 2016; Accepted September 18, 2016

ABSTRACT

Inflammatory processes and androgen signaling are critical for the growth of prostate cancer (PC), the most common cancer among males in Western countries. To understand the importance of potential interplay between pro-inflammatory and androgen signaling for gene regulation, we have interrogated the crosstalk between androgen receptor (AR) and NF-κB, a key transcriptional mediator of inflammatory responses, by utilizing genome-wide chromatin immunoprecipitation sequencing and global run-on sequencing in PC cells. Co-stimulation of LNCaP cells with androgen and pro-inflammatory cytokine TNFα invoked a transcriptome which was very distinct from that induced by either stimulation alone. The altered transcriptome that included gene programs linked to cell migration and invasiveness was orchestrated by significant remodeling of NF-κB and AR cistrome and enhancer landscape. Although androgen multiplied the NF-κB cistrome and TNFα restrained the AR cistrome, there was no general reciprocal tethering of the AR to the NF-κB on chromatin. Instead, redistribution of FOXA1, PIAS1 and PIAS2 contributed to the exposure of latent NF-κB chromatin-binding sites and masking of AR chromatin-binding sites. Taken together, concomitant androgen and pro-inflammatory signaling significantly remodels especially the NF-κB cistrome, reprogramming the PC cell transcriptome in fashion that may contribute to the progression of PC.

INTRODUCTION

Prostate cancer (PC) is the most common malignancy among men worldwide, leading to substantial morbidity and mortality. The development and progression of the PC are androgen-dependent processes, and androgen deprivation is a standard treatment for the disease. Frequently however, PC progresses to androgen-independent, castration resistant PC. The mechanisms involved in the development of the resistance are poorly understood (1,2), but mutations or amplification of androgen receptor (AR) gene or activation of AR protein through other signal transduction pathways have been implicated. AR is an androgen-activated transcription factor (TF) that regulates gene programs mandatory for the male phenotype. In neoplastic prostate cells, the AR regulates important cellular growth and survival programs, and despite the apparent androgen-independency of castration resistant PCs, the AR-mediated signaling remains critical for the growth and survival of the majority of these tumors and the AR is thus a major drug target in the disease (3).

Even if dysregulation of AR signaling is the most important single cause of PC, it is essential to notice that androgen signaling does not function in isolation, but in connection with other signaling pathways. In the PC context, pro-inflammatory signaling pathway integrated at transcription level by nuclear factor κB (NF-κB) is of special interest. NF-κB is a family of five structurally-related TFs, p50, p52, c-Rel, RelA/p65 and RelB that form functional homo- and heterodimers. The term NF-κB commonly refers to p50-p65 heterodimer which is the major NF-κB complex in most cell types (4). A variety of signals, including tumor necrosis factor (TNF) α and other pro-inflammatory cytokines, rapidly activate the NF-κB to regulate its target genes. TNFα exerts a variety of functions in inflammation, cell differentiation, cell proliferation and cell death. In addition to immune cells that can be infiltrated into tumor microenvironment,

*To whom correspondence should be addressed. Tel: +358 40 591 0692; Email: jorma.palvimo@uef.fi
†These authors contributed equally to the paper as first authors.

TNFα is produced by several other cell types, including PC cells (5). Interestingly, increased levels of TNFα in PC correlate with a poor disease prognosis (6). Moreover, the NF-κB pathway is often constitutively activated in cancers, stimulating cell proliferation, inhibiting apoptosis and promoting metastasis and angiogenesis (7). In PC, the NF-κB may also promote resistance to androgen deprivation (8,9).

In addition to the TF's cognate DNA-binding sites, RNA polymerase II (Pol II) and general transcription machinery, transcriptional regulation requires a number of TF-interacting coregulator proteins, coactivators and corepressors (10,11). Protein inhibitor of activated STAT (PIAS) proteins 1–4 can interact with and coregulate several TFs, including the AR and the NF-κB (12–15). PIAS1 for example can either as an AR coactivator or a corepressor, depending on the AR target gene and it can also influence the distribution of AR on chromatin (13). PIAS1 is interestingly overexpressed in PC (16), and elevated PIAS1 levels predict a shorter relapse free time in patients (17). The PIAS1 also interacts with the NF-κB, with TNFα activating the PIAS1 for rapid repression of inflammatory gene activation (18). The biological role of PIAS1 in NF-κB signaling is also supported by studies in mice where disruption of *Pias1* results in elevated expression of a subset of NF-κB-dependent genes (19).

Also other sequence-specific TFs, such as 'pioneer factor' forkhead box protein A1 (FOXA1), that bind to close proximity to AR's DNA-binding sites can have an important role in the regulation of AR function. The occupancy of FOXA1 on chromatin can either facilitate or prevent binding of AR to chromatin (20,21). As in the case of PIAS1, the level of FOXA1 in PC cells significantly contributes to the AR-regulated transcription program, and high levels of FOXA1 in prostate are usually linked to a poor outcome in PC (22,23).

Since inflammatory processes and perturbations in the AR signaling are important, but still poorly understood events in PC, deeper knowledge of the putative crosstalk between the AR and the NF-κB is important for better understanding of the transcription programs promoting the growth of PC. In this work, we utilized chromatin immunoprecipitation sequencing (ChIP-seq) together with global nuclear run-on sequencing (GRO-seq) to decipher the effects of simultaneous androgen and TNFα signaling on the AR and the NF-κB cistrome and gene programs in LNCaP PC cells. Based on our genome-wide analyses, there is no simple mutual transcriptional interference between the AR and the NF-κB as suggested previously, but especially the androgen signaling can significantly remodel the TNFα-induced NF-κB cistrome by exposing latent NF-κB-binding sites. The remodeling was not generally mediated by AR tethering to NF-κB on chromatin, but by androgen and TNFα-triggered genomic redistribution of FOXA1 and PIAS1 and PIAS2, Notably, the crosstalk between the androgen and the TNFα signaling lead to reprogramming of PC cell enhancer landscape and transcriptome in a fashion that is likely to influence prostate carcinogenesis.

MATERIALS AND METHODS

Cell culture and treatments

LNCaP cells (from ATCC) were grown in RPMI1640 (Gibco) supplemented with 10% fetal bovine serum (FBS), 1% penicillin/streptomycin and 2 mM L-glutamine. In signal induction experiments cells were maintained in RPMI 1640 medium with 10% charcoal-stripped FBS for 2 days to deplete androgen actions and then exposed to vehicle (DMSO), DHT (5α-dihydrotestosterone, 100 nM, Steraloids Inc.), TNFα (1000 U/ml, a kind gift from prof. Claude Libert, Ghent University) or both DHT and TNFα. In proliferation assay, the cell numbers were counted using Scepter 2.0 (Merck Millipore).

Antibodies

Antibodies used for immunoblotting and ChIP-seq were rabbit polyclonal anti-AR (24), rabbit polyclonal anti-p65 (Santa-Cruz Biotechnology, sc-372), rabbit polyclonal anti-FOXA1 (Abcam, ab23738), rabbit monoclonal anti-PIAS3+PIAS1+PIAS2 (Abcam, ab77231) and mouse monoclonal anti-tubulin (Santa-Cruz Biotechnology, sc-5286). Standard protocols for immunoblots were used as (25). The appropriate secondary antibodies were from Invitrogen and chemiluminescence detection reagents from Pierce.

RNA interference and RT-qPCR

FOXA1 was silenced as described (15,26). Briefly, cells were reverse-transfected with siRNAs against FOXA1 (siFOXA1) or non-targeting control (siNON) siRNA (Dharmacon; On-TARGETplus pool and non-targeting pool) using Lipofectamine RNAiMAX transfection reagent (Life Technologies). Four days after transfection, cells were treated, total cellular RNA was collected (TriPure reagent; Roche) and cDNA was synthesized with oligo dT primers (Transcriptor First Strand cDNA synthesis Kit; Roche). Three biological replicates were analyzed using LightCycler 460 SYBR GREEN I reagent and LightCycler 480 polymerase chain reaction (PCR) apparatus (Roche). GAPDH was used to normalize amounts of mRNA between samples, and vehicle-treated siNON sample to get the relative mRNA levels in each sample. Statistical significance of the changes in RT-qPCR data were analyzed in GraphPad PRISM using one-way ANOVA. Primer sequences are available upon request.

ChIP-seq

ChIP-seq was performed according to a published protocol (27) with minor modifications and two biological replicates. Briefly, the cells grown on 10-cm dishes were fixed in 1 % (v/v) formaldehyde 10 min at room temperature. Chromatin was fragmented to ∼200–400 bp using sonication (Bioruptor UCD-300, Diagenode). Antibodies were coupled to protein-A- beads (Millipore), fragmented chromatin was incubated with antibody-coupled beads overnight, washed, eluted and de-cross-linked in the presence of proteinase K (Fermentas). Chromatin fragments were purified using MinElute columns (Qiagen), ChIP-seq libraries were

prepared using NEBNext kit (New England Biolabs) and sequenced with HiSeq 2000 at EMBL GeneCore (Heidelberg, Germany). Fragmented de-cross-linked chromatin was used as a control. Previously published ChIP-seq data for H3K4me1 and H3K27me3 histone marks were used (GSE62492 (28)).

Sequenced raw reads were quality controlled using FastQC and quality filtered using FASTX-toolkit as described (29) before reads were mapped to human genome (hg19) using bowtie keeping only uniquely mapping reads. Read counts are in Supplementary Table S1. Initial binding sites were defined for both biological replicates against control sample using findPeaks program of HOMER package (30) with default settings. Binding sites found in both biological replicates were considered representative for the given condition and used in the analysis. Signal matrixes for heat maps and line profiles were done in HOMER and visualized using imageJ (31) and R (www.R-project.org). Chromatin tracks were done in IGV and assembled in Photoshop (Adobe). DNA motif discovery was done with findMotifsGenome tool of the HOMER package.

GRO-seq

Samples of two biological replicates were processed essentially as described (32). Briefly, nuclei from approximately 10 million cells were collected in swelling buffer, run-on reactions were done in the presence of Br-UTP, RNA was isolated using TRIZOL-LS reagent (Life Technologies) and labeled RNA molecules were affinity purified using agarose-conjugated anti-BrdU (sc32323AC, Santa Cruz Biotechnology, Texas, USA). Labeled RNAs were processed for next-generation sequencing with minor modifications from a published protocol (33). Samples were sequenced with HiSeq 2000 at EMBL GeneCore. GRO-seq reads were quality controlled using FastQC and FASTX-toolkit (minimum 97% of bps over quality score 10). Poly-A tails were trimmed, and smaller than 25 nt long reads and reads that mapped to rRNA were discarded. Remaining reads were mapped to reference human genome (hg19) using bowtie ($v = 2$, $m = 3$, $k = 1$). Read counts are in Supplementary Table S1. Gene body (+250 bp to transcription termination site (TTS)) transcription was analyzed using HOMER. Gene body RPKM cutoff >0.5 was used to differentiate between transcribed and non-transcribed genes. Differential expression (FDR < 0.01 and $\log_2$FC > 1or < −1 as cutoffs) for transcribed genes was analyzed using edgeR (34). To identify biological processes enriched for differentially expressed genes, the data were analyzed using Ingenuity Pathway Analysis® (IPA, www.ingenuity.com). A core analysis was first performed with three distinct lists (DHT-regulated genes, TNFα-regulated genes and D+T-regulated genes) and the results were then compared to identify differentially regulated biological processes (Z-value cut-off 2, *P*-value < 0.05). In order to determine transcribed enhancers, GRO-seq libraries were combined and intergenic transcripts (over 10 kb from the TTS to avoid gene read through artifacts) were determined using findPeaks in HOMER (style = groseq, tssFold = 3, bodyFold = 3, minBodySize = 200). Chromatin loci where two opposing-strand transcripts were identified no more than 1 kb apart from each other, were considered eRNA enhancers. Enhancers were associated with the nearest genes in HOMER. Transcription was measured from 2-kb window centered to eRNA enhancers. Kruskal–Wallis statistical test and Dunn's post-test were done in GraphPad Prism software to evaluate statistical significance of the changes in transcription at eRNA enhancers, ARBs and p65Bs.

Accession numbers

The high-throughput sequencing data are submitted to the Gene Expression Omnibus (GEO) database, www.ncbi.nlm.nih.gov/geo (accession no. GSE83860).

RESULTS

LNCaP prostate cancer cells respond to both androgen and TNFα

To analyze how PC cells respond to activation of androgen and pro-inflammatory signaling, we exposed LNCaP PC cells to androgen DHT or TNFα or both of them (D+T) and followed how the exposures affect cell proliferation. Androgen induced, while TNFα inhibited the proliferation of LNCaP cells, respectively (Supplementary Figure S1). When both signaling pathways were simultaneously activated, TNFα blunted the growth stimulatory effect of androgen, leading to cell proliferation that did not significantly differ from that in vehicle-treated cells. Our results are in line with a previous report showing that TNFα inhibits DHT-induced proliferation of LNCaP cells (35). These results indicate that in addition to androgen signaling, the growth of LNCaP cells respond to TNFα signaling, but in a fashion that is the opposite to androgen signaling.

Crosstalk between androgen and TNFα signaling results in opposite effects on the chromatin binding of AR and p65

To explore the crosstalk between androgen and TNFα pathway on the genome-wide level, we analyzed chromatin binding of the AR and the p65 in DHT- and/or TNFα-treated LNCaP cells using ChIP-seq. DHT treatment resulted in extensive loading of AR onto chromatin (19,672 AR chromatin-binding sites, ARBs) (AR DHT in Figure 1A), while TNFα or vehicle did not have a marked effect on AR binding. Combined treatment with DHT and TNFα lead to a substantial rearrangement of AR chromatin binding; the majority of the ARBs with strong ChIP-seq signal were preserved (11 320; AR D+T in Figure 1A), but interestingly a significant proportion (8352) of weaker ARBs were lost and some new ARBs were gained (704). Heat map and line profile analyses suggested that some of the ARBs in D+T treatment were also bound by p65 under the same conditions (p65 D+T in Figure 1A). H3K4me1, a histone mark typically associated with enhancer regions (36), but not H3K27me3, a mark of inactive chromatin, was surrounding the ARBs in all peak fractions, especially those shared with DHT and D+T. The androgen-induced increase in H3K4me1 signal suggests that many of the ARBs correspond to androgen-induced enhancers. Analysis of known DNA-binding motifs showed that AR motif (ARE) was most abundant at ARBs shared between DHT and D+T

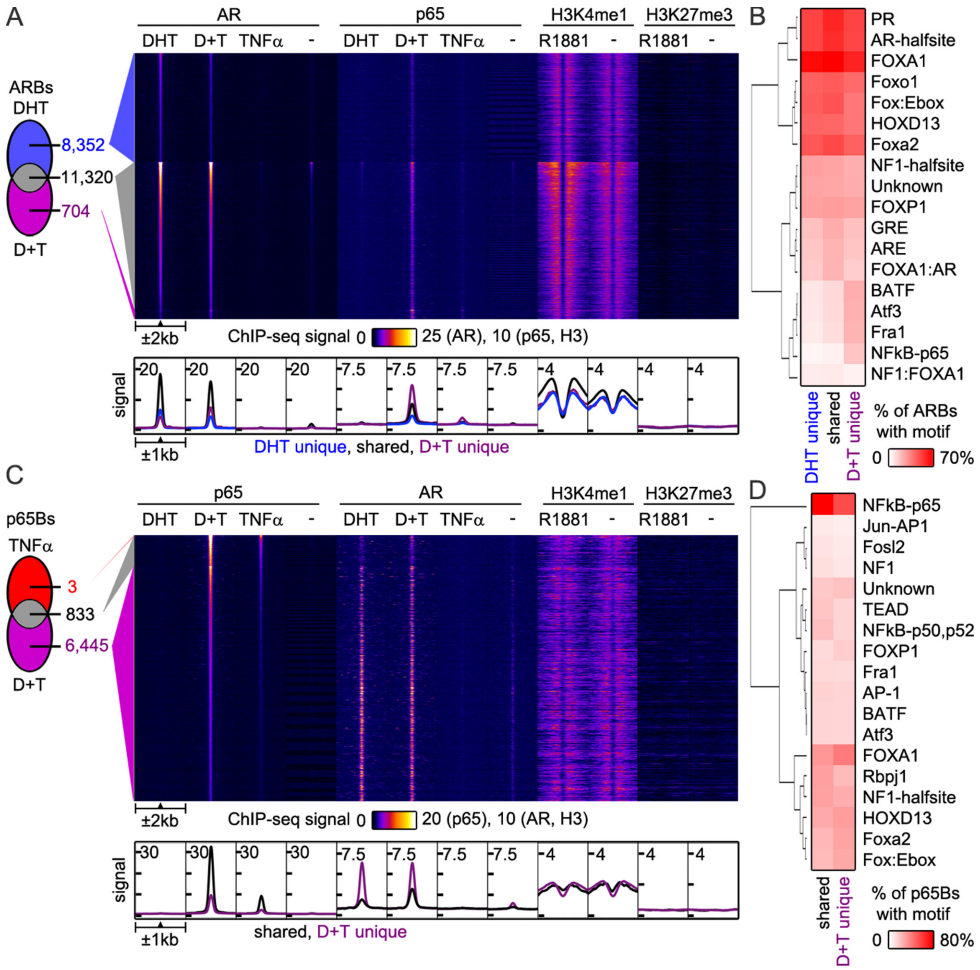

Figure 1. Crosstalk between androgen and TNFα signaling is reflected in the chromatin binding of AR and p65. ChIP-seq was used to analyze the chromatin binding of the androgen receptor (AR) and the p65 (activating subunit of NF-κB) in LNCaP cells treated 2 h with DHT (100 nM), TNFα (1000 U/ml) or both (D+T). (**A**) Venn diagram showing overlap of ARBs in cells exposed to DHT or D+T. Heat map showing ChIP-seq signals of AR and p65 in DHT, TNFα, D+T or vehicle (DMSO, −) treatment and H3K4me1 and H3K27me3 histone marks (28) in androgen (R1881) and vehicle (−) treatment at ±2 kb window surrounding ARBs. ChIP-seq intensities are normalized to 10^7 reads and shown using false-color scale (intensity increases from darker to lighter colors). Line profiles show average ChIP-seq signal intensities at ±1 kb area surrounding the peak centers at ARBs unique to DHT (blue), D+T (purple) or shared between two peak populations (black). (**B**) Hierarchical clustering of enriched DNA-binding motifs of different ARB categories. Percentage of ARBs with motif is shown with shades of red. (**C**) Venn diagram showing overlap of p65Bs in cells exposed to TNFα or D+T. ChIP-seq signals in heat map are same as above shown at ±2 kb window surrounding p65Bs. Line profiles show average ChIP-seq signal intensities at ±1 kb area surrounding the peak centers of p65Bs shared between TNFα and D+T (black) or the ones unique to D+T (purple). (**D**) Hierarchical clustering of enriched DNA-binding motifs of different p65B categories. Percentage of motifs in p65Bs is shown with shades of red.

treatment, and FOXA1 motif was highly abundant among all ARBs (Figure 1B). NF-κB-p65 motif was significantly enriched only at D+T unique ARBs.

As anticipated, TNFα induced chromatin binding of p65 in LNCaP cells (836 binding sites; p65 TNFα in Figure 1C), while no binding was observed in DHT- or vehicle-treated cells. Compared to TNFα alone, D+T treatment resulted in 8-fold increase in p65 chromatin-binding sites (p65Bs) (7278; p65 D+T in Figure 1C), including practically all binding sites observed in TNFα treatment alone. This change was likely to be a result of enhanced chromatin binding of p65, as judged by a substantial increase in the overall ChIP-seq signal in D+T compared to TNFα (Figure 1C heat map and line profile). Heat map analysis suggested that some, especially D+T unique, p65Bs were bound by AR in DHT and D+T treatment (AR DHT and D+T in Figure 1C). H3K4me1 was enriched at the vicinity of p65Bs (Figure 1C). Unlike at the ARBs, there was no androgen-induced increase in H3K4me1 signal at the p65Bs, suggesting that the p65 is not binding to androgen-activated enhancers. NF-κB motif was most abundant at p65Bs shared between TNFα and DHT treatment (Figure 1D). Interestingly, FOXA1 motif that was highly enriched at the ARBs was more abundant at D+T unique p65Bs than at those shared with TNFα (Figure 1D). A closer inspection of ARB and p65B co-occurrence showed that ∼1500 of ARBs and p65Bs (∼12% of the ARBs and ∼20% of p65Bs) overlapped in D+T treatment. These data point to interesting cross-talk between androgen and TNFα signaling at the level of chromatin binding of AR and p65.

Androgen and TNFα signaling induce chromatin binding of FOXA1 and PIAS1/PIAS2

A low co-occurrence of the ARBs and the p65Bs suggests that D+T-induced changes in AR and p65 cistromes are largely mediated through indirect mechanisms. A possible mechanism explaining the D+T-induced changes in the AR and the p65 chromatin binding could be an interference with common coregulators, such as PIAS1, or interaction with pioneer factors, such as FOXA1, whose involvement in chromatin binding of p65 is suggested by our DNA motif analysis.

To analyze if FOXA1 and PIAS proteins are involved in the crosstalk between androgen and TNFα signaling, we mapped their chromatin binding in DHT- and/or TNFα-treated LNCaP cells using ChIP-seq. Based on our mRNA expression and siRNA-silencing coupled to immunoprecipitation and immunoblotting analyses, the PIAS3+PIAS1+PIAS2 antibody used for ChIP-seq mainly recognizes PIAS family members PIAS1 and -2 (14) that are referred to as PIAS1+2 from now on (Supplementary Figure S2). As shown in heat map (Figure 2A), FOXA1 was abundantly found at all ARBs and PIAS1+2 mostly at the ARBs shared between DHT and D+T treatment. DHT as well as D+T treatment enhanced FOXA1 and PIAS1+2 binding particularly at the ARBs shared between DHT and D+T treatment (Figure 2A line profile and Figure 2B), suggesting that the AR is generally affecting chromatin binding of these factors. The overlap of AR peaks with FOXA1 and PIAS1+2 under different conditions is shown in Supplementary Figure S3A.

Analysis of p65Bs revealed that there was ≥50% co-occurrence of FOXA1 with p65 both in TNFα and D+T treatment (Supplementary Figure S3B). The co-occurrence of PIAS1+2 with p65 was also prominent: ∼70% overlap in TNFα and >34% overlap in D+T treatment (Supplementary Figure S3B). Interestingly, TNFα and D+T treatment induced chromatin binding of FOXA1 and PIAS1+2 at the p65Bs in general (Figure 2C line profile and Figure 2D), implying that FOXA1 and PIAS1+2 function as TNFα-recruited factors at p65-targeted enhancers.

These data indicate that the activation of the AR and the p65 leads to redistribution of the FOXA1 and the PIAS1 and -2 coregulator proteins on chromatin, suggesting the involvement of the pioneer factor and the coregulator proteins in genomic crosstalk between androgen and TNFα signaling.

FOXA1 modulates p65 chromatin binding and TNFα response

Next, we analyzed if FOXA1 influences the chromatin binding and function of p65. To this end, we used ChIP-seq to analyze the p65 cistrome after silencing of FOXA1 by RNAi. Transfection of FOXA1-specific siRNAs effectively depleted the FOXA1 protein in LNCaP cells as assessed by immunoblotting (Figure 3A). Unexpectedly, control siRNA transfection (siNON) increased the number of TNFα-induced p65Bs by >10-fold compared to the situation in non-silenced cells (8838 versus 836), which is likely to be due to a transfection-induced cell stress response. Nevertheless, FOXA1 silencing caused a massive shift in the TNFα-induced chromatin binding of p65; 4339 novel p65Bs appeared and 5343 disappeared upon the FOXA1 depletion, while 3495 p65Bs remained stable (Figure 3B). The majority of the p65Bs that were lost upon the FOXA1 depletion showed co-occupancy with FOXA1 (83%) and PIAS1+2 (83%) in TNFα-treated non-silenced cells. In contrast, only a minority of the p65Bs that emerged in FOXA1-depleted cells had FOXA1 (12%) or PIAS1+2 (27%) in TNFα-treated non-silenced cells. Quantification of the ChIP-seq signals at different p65B groups confirmed the strong binding of FOXA1 and PIAS1+2 at FOXA1 silencing-sensitive p65Bs (Figure 3C). In line with above results, DNA motif analysis showed a high enrichment of FOXA1 motif at FOXA1 depletion-sensitive TNFα-induced p65Bs (64% of peaks; Figure 3D), whereas NF-κB motif was enriched to a much lesser extent (22%). Occurrence of these motifs was reversed at FOXA1 depletion-insensitive p65Bs (NF-κB, 70%; FOXA1, 23%) and FOXA1 depletion-gained p65Bs (NF-κB, 57%; FOXA1, no enrichment) (Figure 3D). Figure 3E shows examples of cancer-linked genes that lost TNFα induction (*VEGFA*) or became TNFα inducible (*OLA1*) upon FOXA1 depletion.

These results suggest that FOXA1 is able to function as a pioneer factor for p65 in PC cells and that the FOXA is also able to mask binding of p65 at a large number of NF-κB motif-containing chromatin sites.

Concomitant androgen and TNFα signaling invokes a distinct pattern of enhancer activity

To analyze if changes in AR and p65 chromatin binding are reflected in enhancer activity, we used GRO-seq to determine enhancer RNA (eRNA) transcription, which has been shown to reflect with the activity of enhancers (36,37). DHT-, TNFα- and D+T-induced transcription of canonical bi-directional short eRNA transcripts was apparent at many ARBs and p65Bs (Figure 4A). Quantification of eRNA transcription (±2 kb region from the center of ARBs/p65Bs) at intergenic ARBs and p65Bs showed that also the D+T unique ARBs and p65Bs represent inducible, functional enhancers (Figure 4B and C).

Next, we defined intergenic regions that had opposing transcripts within 1 kb of each other as eRNA enhancers (Figure 4D), yielding 2092 intergenic bi-directional eRNA-producing enhancers (Figure 4E). Overall, DHT and TNFα treatments induced different sets of enhancers, as shown by negligible correlation between DHT-induced and TNFα-induced changes in enhancer transcription (Spearman's correlation coeffient $[r_s] = 0.153$; P-value $< 2.11 \times 10^{-12}$; Figure 4E). However, DHT-induced changes in enhancer transcription were moderately ($r_s = 0.523$; P-value $< 1 \times 10^{-44}$) and TNFα-induced ones strongly ($r_s = 0.715$; P-value $< 1 \times 10^{-44}$) correlated with the changes observed in D+T treatment (Figure 4E). D+T treatment resulted in the highest number of differentially regulated enhancers (506 up, 345 down), of which ∼60% and ∼30% were similarly regulated in TNFα and DHT treatment, respectively. Enhancers that were upregulated by any of the treatments (UP in DHT, TNFα or D+T) or downregulated by DHT or TNFα (DOWN in DHT or TNFα) associated with genes

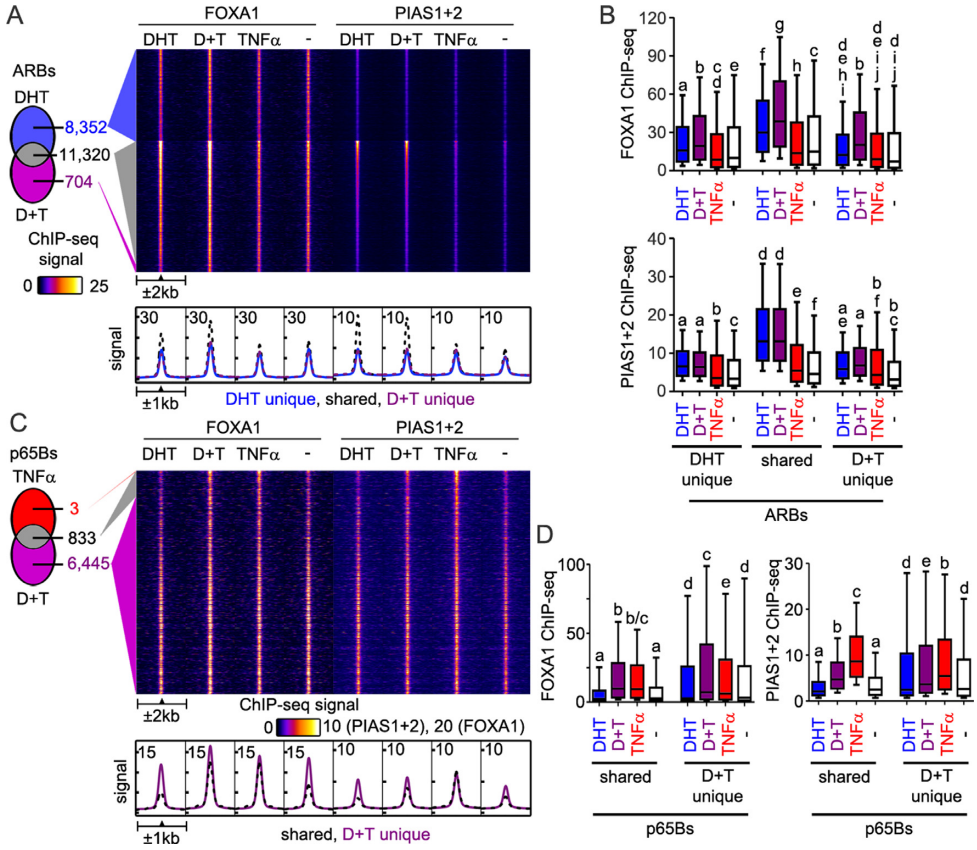

Figure 2. TNFα induces FOXA1 and PIAS1/2 binding at p65 chromatin-binding sites. Chromatin binding of the FOXA1 and the PIAS proteins was analyzed with ChIP-seq in LNCaP cells treated as in Figure 1. (**A**) False-color scale heat map (intensity increases from darker to lighter colors) of FOXA1 and PIAS1+2 ChIP-seq signal intensities at different ARB groups. Line profile showing FOXA1 and PIAS1+2 average ChIP-seq signals at ARBs unique to DHT (blue), unique to D+T (dashed purple line) or shared with both ARB groups (dashed black line). (**B**) Boxplot of FOXA1 (upper panel) and PIAS1+2 (lower panel) ChIP-seq signals in DHT (blue), TNFα (red), D+T (purple) and vehicle (white) conditions at ±100 bp region of different ARB groups. Statistically different groups are given unique labels (Kruskal–Wallis test, Dunn's post-test, $P < 0.05$). Whiskers in boxplot mark 10% and 90% of the data and the line represents the median. (**C**) Heat map of FOXA1 and PIAS1+2 at different p65B groups. Signals are the same as in A. Line profile of average FOXA1 and PIAS1+2 ChIP-seq signals at D+T unique (purple) or TNFα D+T shared (dashed black line) p65Bs. (**D**) Boxplot of FOXA1 (left) and PIAS1+2 (right) signals at different p65B groups. Color coding and analysis are the same as in B.

that were upregulated or downregulated in the corresponding treatment, respectively (Figure 4F and G).

In conclusion, DHT and TNFα signaling affects about half of all identified enhancers in LNCaP cells and the crosstalk between androgen and TNFα signaling results in a distinct enhancer landscape.

Androgen-regulated transcriptome is altered by TNFα

To confirm the functional relevance of the crosstalk between androgen and TNFα signaling, we analyzed transcription in LNCaP cells exposed to DHT, TNFα or D+T using GRO-seq. Compared to vehicle treatment, 3454 genes were differentially transcribed in at least one of the treatments (Figure 5A; FDR < 0.01). Transcriptional changes in DHT treatment were moderately ($r_s = 0.513$; P-value $< 1 \times 10^{-44}$) and in TNFα treatment strongly ($r_s = 0.781$; P-value $< 1 \times 10^{-44}$) correlated with those in D+T treatment (Figure 5B), while correlation between DHT- and TNFα-induced changes in gene transcription was negligible ($r_s = 0.129$; P-value $< 2.53 \times 10^{-14}$). DHT treatment lead to differential transcription of 1118 genes (736 up, 382 down) of which ∼65% (730/1118) were similarly regulated in D+T-treated cells (Figure 5C and D). TNFα treatment altered transcription of 2456 genes (1677 up, 779 down) and ∼65% (1599/2456) of these were similarly regulated in D+T treatment (Figure 5C and D). Notably, 445 genes were uniquely regulated by D+T treatment (174 up, 271 down).

To understand the potential effects of these transcriptional changes for cellular functions, we subjected differentially transcribed genes to biological function analysis using Ingenuity Pathway Analysis. Compared to control cells, 202 disease and biological function pathways were predicted to be activated (Z-score > 2; P-value < 0.05) or repressed (Z-score < −2; P-value < 0.05) in at least one of the treatment conditions (selected pathways shown in Figure 5E; full list of enriched pathways in Supplementary Table S2). Interestingly, 20 of these pathways were significantly upregulated and 3 of them downregulated merely in D+T treatment (selected ones marked in red in Figure 5E). The D+T treatment unique functional pathways included cell movement of cancer/tumor cells, migration of cancer cells, differentiation of bone/bone cells and vasculogenesis. In addition, 33 pathways showed more pronounced activation and

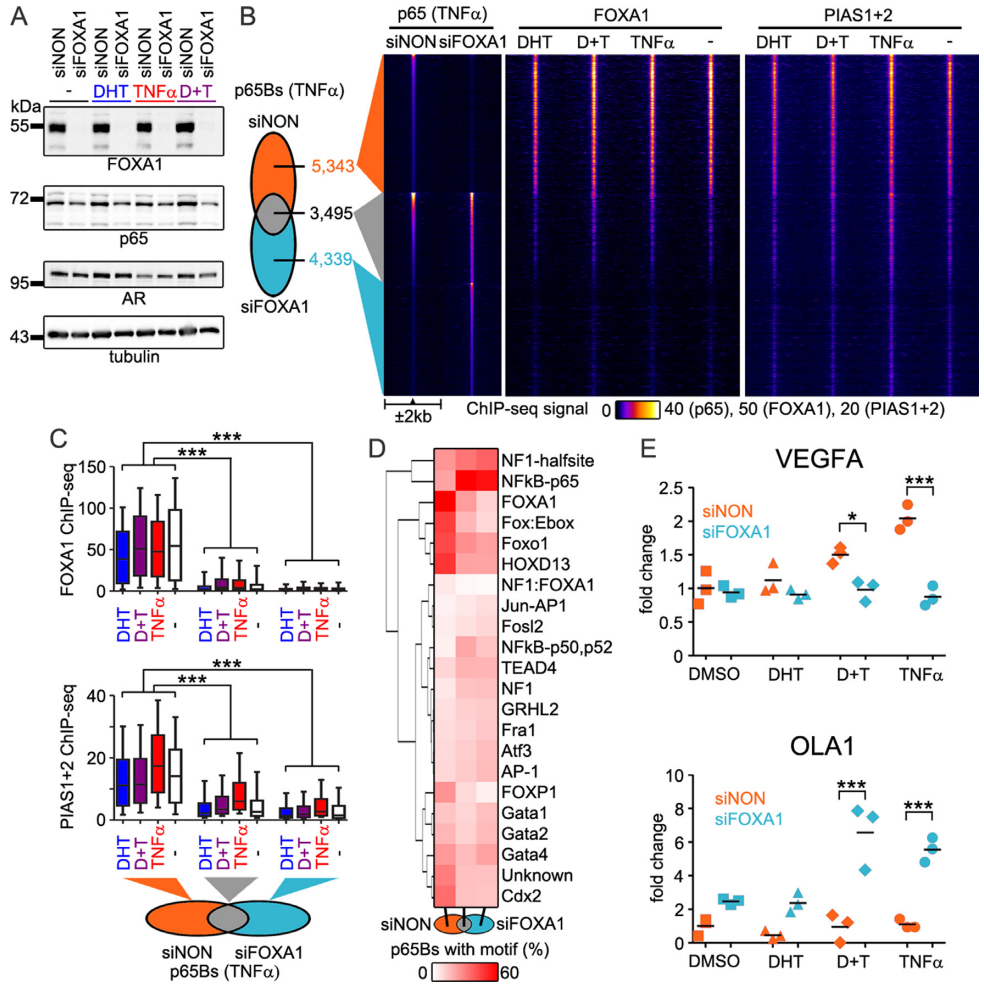

Figure 3. FOXA1 modulates chromatin binding of p65. The role of FOXA1 in p65 chromatin binding was analyzed in FOXA1 silenced cells (siFOXA1) and control siRNA transfected (siNON) cells treated with TNFα using ChIP-seq. (**A**) Immunoblotting of FOXA1 silenced (siFOXA1) and control (siNON) cells treated 2 h with DHT, TNFα, both (D+T) or vehicle (−) using anti-FOXA1, anti-p65, anti-AR and anti-tubulin antibodies. (**B**) Venn diagram showing overlap of p65Bs in TNFα-treated siNON and siFOXA1 cells and false-colored heat map showing ChIP-seq signal intensities of p65 (siNON and siFOXA1), FOXA1 (non-silenced) and PIAS1+2 (non-silenced) at ±2 kb window centered at p65Bs. (**C**) Boxplot of FOXA1 (upper panel) and PIAS1+2 (lower panel) signals in DHT (blue), TNFα (red), D+T (purple) or vehicle (white) treatments at different p65B groups. Whiskers in boxplot mark 10% and 90% of the data and the line represents the median. (**D**) Hierarchical clustering of DNA-binding motif occurrences in p65Bs unique to siNON or siFOXA1 or shared with two treatments. (**E**) Effect of FOXA1 depletion on the gene expression of *VEGFA* and *OLA1* genes. RT-qPCR results of DHT-, TNFα-, D+T- or vehicle-treated siNON (orange) and siFOXA1 (light blue) transfected cells were normalized to *GAPDH* mRNA levels and fold changes were calculated in reference to siNON in vehicle treatment. Three biological replicates and the average value are shown. All significant changes between siNON and siFOXA1 pairs within a single treatment are marked with stars (one-way ANOVA; **P*-value < 0.01, ****P*-value < 0.001).

2 more pronounced repression in D+T treatment compared to other treatments (selected ones marked in orange in Figure 5E). These included many cancer-linked biological functions, including cell viability, cell survival and proliferation of tumor cells.

These transcriptome data indicate that DHT and TNFα invoke largely different gene programs in PC cells. Interestingly, simultaneous activation of androgen and TNFα signaling leads to activation of distinct functional pathways as well as stronger regulation of multiple functional pathways many of which are relevant for cancer progression.

DISCUSSION

The development and progression of PC are AR-dependent processes, but a substantial evidence also links a chronic inflammation with the PC progression (38). Although the PC cells themselves may produce pro-inflammatory cytokines, such as TNFα, the majority of the inflammatory effects in PC are thought to be mediated through tumor-infiltrating immune cells or reciprocal interaction between immune and PC cells (39). Previously, inflammatory signaling, especially via NF-κB pathway, has been suggested to antagonize AR signaling in PC cells and in many cases the activity of AR and NF-κB signaling pathways were thought to be mutually exclusive (40,41). Moreover, simple reporter gene assays suggested that there is a mutual and direct transcriptional interference between the AR and the p65, in which coregulator proteins may also play a role (42,43).

Here, we studied the crosstalk between androgen and TNFα-induced inflammatory signaling in PC cells in an un-

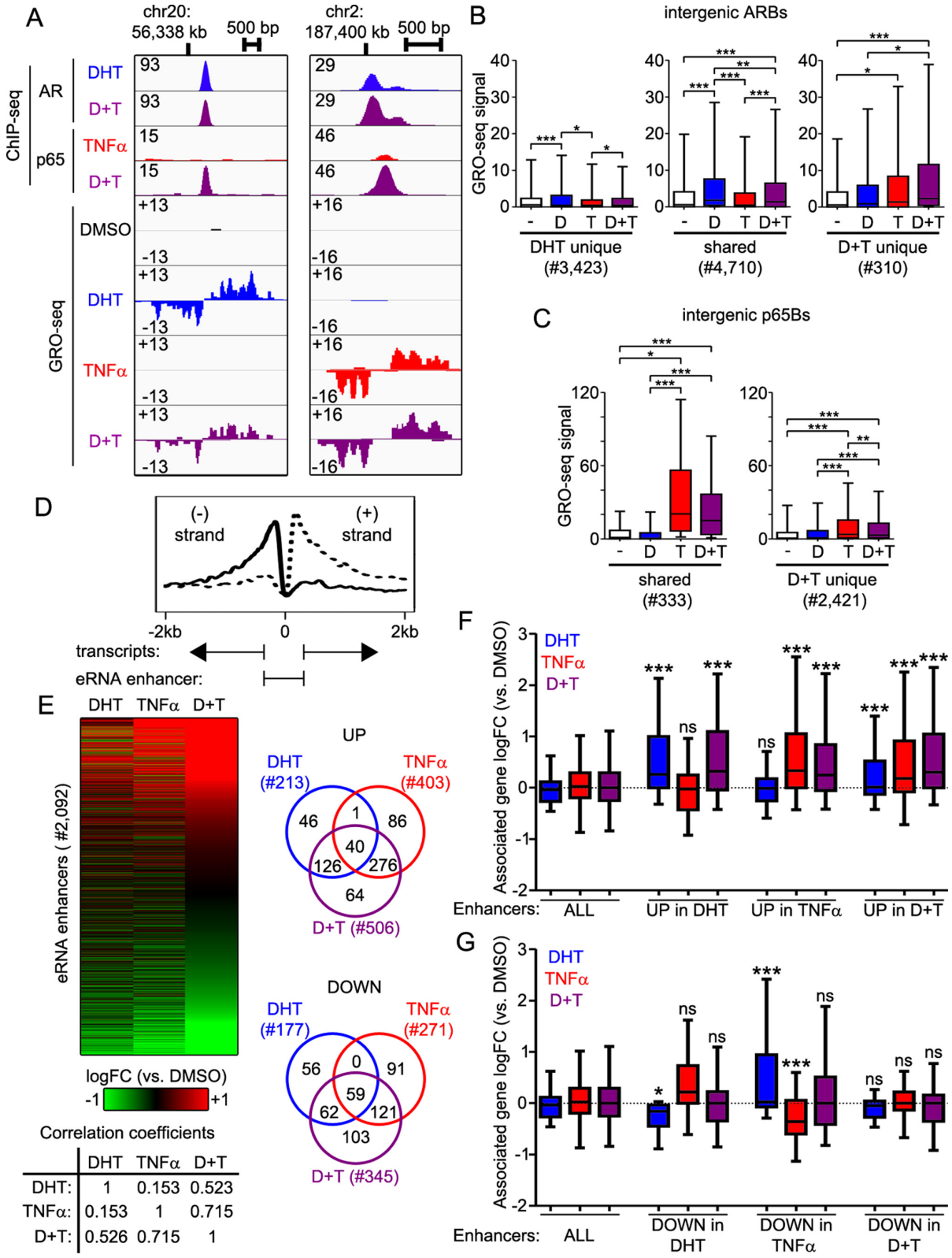

Figure 4. Interplay between androgen and TNFα signaling leads to a distinct enhancer activity landscape. GRO-seq was used to map transcription in LNCaP cells treated for 4 h with vehicle (black), DHT (blue), TNFα (red) or both (D+T, purple). (**A**) The visualization of AR and p65 ChIP-seq and GRO-seq (plus- and minus-strands) signals at two intergenic loci show DHT and TNFα-induced binding of AR and p65, and induction of bi-directional transcription. Numbers depict the maximum signals. (**B**) Boxplot of GRO-seq signals at control (−, white), DHT (D, blue), TNFα (T, red) and D+T (purple) treatment at different intergenic ARB groups (DHT unique, shared and D+T unique) ±2 kb from the center of ARBs. (**C**) Boxplot of GRO-seq signals in control (white), DHT (blue), TNFα (red) and D+T (purple) treatment at different intergenic p65B groups (D+T unique and TNFα shared) ±2

biased, genome-wide fashion by following chromatin binding of AR and p65, and by analyzing the resulting changes in enhancer activation and gene transcription. Compared to androgen or TNFα alone, simultaneous activation of androgen and TNFα signaling lead to massive, and opposite, effects on chromatin binding of AR and p65: the AR cistrome was diminished, while the p65 cistrome was amplified. However, only a fraction of the AR- and the p65-binding events on chromatin co-occurred, suggesting that a direct interaction, or tethering, between the AR and the p65 is not a general explanation for the majority of their crosstalk-induced changes in the chromatin binding. Instead, competition or redistribution of other factors, such as pioneer TFs and/or coregulators, that are common to AR and NF-κB is likely to mediate the modulation of AR and NF-κB cistromes. FOXA1 has been dubbed a pioneer TF, as it can prime chromatin and hence dictate and guide the binding of other TFs (44). On the other hand, it has recently become evident that other TFs, such as estrogen receptor (ER) α and glucocorticoid receptor (GR), can also redistribute the FOXA1 on chromatin (45). FOXA1 is abundantly bound at AR chromatin-binding sites (15,46,47), and similarly to the ERα and the GR, we show that the AR can influence the chromatin-binding of the FOXA1. Interestingly, the occupancy of FOXA1 at the ARBs was even more pronounced in PC cells co-stimulated with androgen and TNFα than androgen alone. Our data also provide evidence for the involvement of FOXA1 in the NF-κB-mediated gene regulation in PC cells. Many p65 chromatin-binding sites harbored FOXA1 in unstimulated cells, in support of its pioneer function for NF-κB. The occupancy of FOXA1 increased at the p65 chromatin-binding sites upon stimulation by TNFα, implying that also the p65 can alter the genomic distribution of FOXA1. Interestingly, silencing of FOXA1 in PC cells had a dramatic effect on the chromatin binding pattern of p65, which also altered TNFα-regulated gene expression. In addition to the FOXA1, chromatin binding of PIAS1 and PIAS2 was enhanced by androgen and TNFα, suggesting that both the AR and the p65 are recruiting these coregulator proteins onto PC chromatin. Moreover, PIAS1 has been recently shown to function as a target gene selective AR coregulator that also interacts with the FOXA1 and influences AR chromatin occupancy (15). PIAS1 additionally interacts with the NF-κB, with TNFα activating the PIAS1 via IκB kinase α-mediated phosphorylation for rapid repression of inflammatory gene activation (18,19). As PIAS1 is capable of promoting SUMOylation of both FOXA1 and AR (15,48), also SUMOylation events are likely to contribute the action of FOXA1 and PIAS1 upon TNFα and androgen exposure. These results suggest that both the FOXA1 and the PIAS1/PIAS2 contribute to the altered repertoire of NF-κB and AR chromatin-binding sites during crosstalk between androgen and TNFα signaling.

Transcription analysis revealed that androgen and TNFα signaling largely regulate different sets of enhancers and genes in PC cells. However, simultaneous activation of the two signaling pathways lead to a distinct enhancer activity profile and transcription program, with activation of many cancer-relevant functional pathways. The genes that were particularly or uniquely responsive to the concomitant stimulation of PC cells with androgen and pro-inflammatory cytokine were enriched in biological functions that are important for several cancer-linked biological functions, including tumor cell movement, viability and survival. PCs often metastases to bones, and NF-κB signaling has been shown to contribute to bone metastasis formation (49). Interestingly, the TNFα-induced androgen-modulated genes included genes in bone cell differentiation pathways, such as IL-32, an osteoclast differentiation contributing pro-inflammatory cytokine (50). Activation of the bone differentiation-linked pathways in inflammation could be important for the bone metastasis formation in PC.

There is still scanty information of genome-wide crosstalk between different signal-inducible TFs. Coactivation of GR and NF-κB/p65 has been reported to alter the repertoire of their target genes without strongly affecting the number of GR or NF-κB chromatin-binding sites (51). The coactivation however resulted in appearance of a group of novel GR and NF-κB chromatin-binding sites that were dependent on the mutual tethering of the GR and the NF-κB on chromatin (51). Although we also observed an overlap of a fraction of AR and NF-κB cistromes upon coactivation of AR and NF-κB, the number of coactivation-gained novel AR chromatin-binding sites in PC cells was very small in comparison to that of novel NF-κB sites and they cannot not be explained by the co-occupancy of the AR at these sites. As opposed to direct AR-NF-κB interactions or tethering, our data support the notion that AR-induced chromatin redistribution of FOXA1 and PIAS1 and -2 is involved in the alteration of the NF-κB cistrome. Interestingly, redistribution of coregulators from enhancers by NF-κB was recently shown be important also in the regulation of adipocyte identity genes by TNFα (52). Moreover, TNFα-induced chromatin redistribution of FOXA1 was recently reported to take place in breast cancer cells and, together with NF-κB binding, expose latent ERα binding sites in chromatin (53). In PC cells, the major outcome of the genomic crosstalk between male sex steroid and pro-inflammatory signaling

←

kb from the center of p65Bs. (**D**) Schematic presentation of transcription defined eRNA enhancers. Intergenic eRNA enhancers were defined as regions where two opposing ≥200-bp long intergenic transcripts are found <1 kb apart from each other. (**E**) Heat map of logarithmic fold changes (log_2FC, ±2 kb) of eRNA enhancer in DHT, TNFα and D+T treatments compared to vehicle. Venn diagram showing overlap of up- (UP; $log_2FC > 0.5$, FDR < 0.1) and downregulated (DOWN; $log_2FC < -0.5$, FDR < 0.1) enhancer transcription. The table of Spearman's correlation coefficients of enhancer log_2FC values (P-values $<2.2 \times 10^{-12}$). Boxplots of logarithmic fold change of enhancer-associated genes (log_2FC; compared to vehicle) in DHT (blue), TNFα (red) or D+T (purple) treatments. Genes associated with eRNA enhancers that were upregulated (**F**) and downregulated (**G**) in DHT, TNFα or D+T treatment are shown. Genes associated with all eRNA enhancers (ALL) were not differentially transcribed in any of the treatments. In all boxplots, stars depict P-values (***P-value < 0.001, **P-value < 0.01, *P-value < 0.05, ns = non-significant) of Kruskal–Wallis/Dunn's multiple comparison tests. In gene associations in F and G, significance to equivalent treatment in ALL enhancers is shown. In all boxplots, line represents median and whiskers mark 10% and 90% of the data.

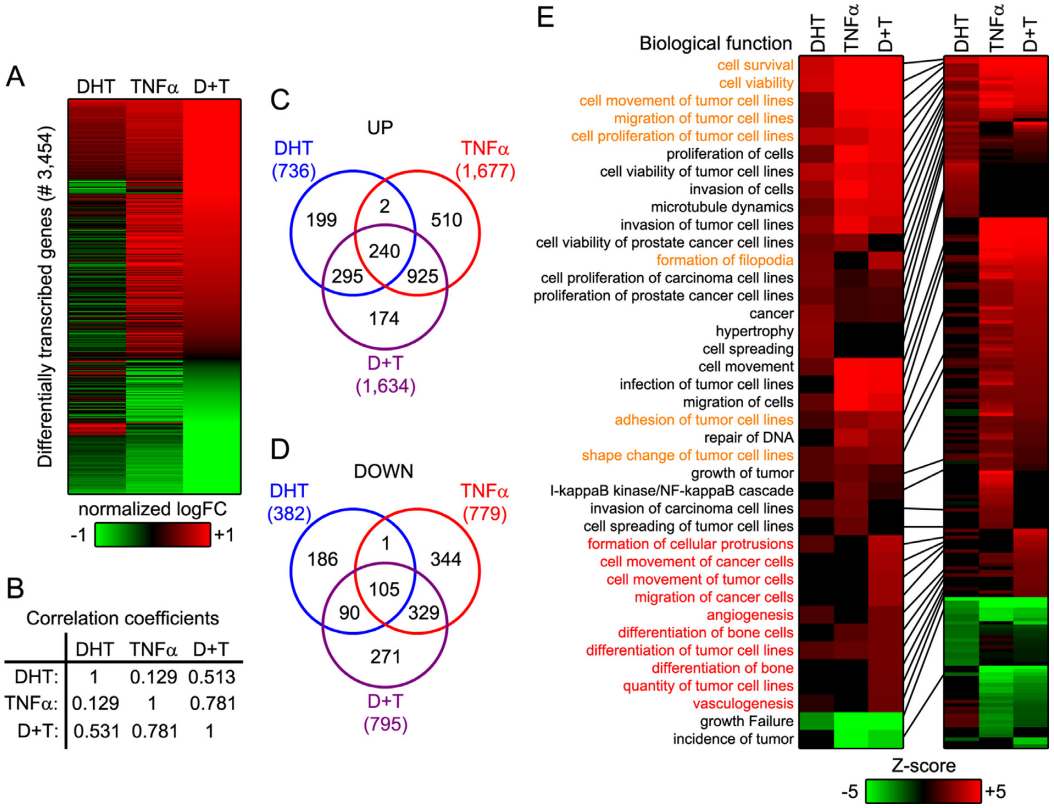

Figure 5. Prostate cancer cell transcriptome is reprogrammed by coactivation of AR and NF-κB. DHT, TNFα and D+T-induced changes in gene transcription were measured using GRO-seq and enrichment of differentially transcribed genes to biological processes was analyzed by Ingenuity Pathway Analysis. (**A**) Heat map of normalized transcription changes in 4 h DHT, TNFα or D+T treatments. Transcription of all treatments compared to vehicle was normalized between maximum and minimum values and all genes that were differentially transcribed in any treatment are shown (FDR < 0.01). (**B**) The table of correlation coefficients of differentially transcribed genes (Spearman's correlation; *P*-values $<2.6 \times 10^{-14}$). (**C** and **D**) Venn diagrams showing overlap of genes that were upregulated (C) or downregulated (D) in DHT (blue), TNFα (red) and D+T (purple) treatments. (**E**) Heat map of changes in activity of disease and biological function pathways. A core analysis was performed in Ingenuity Pathway Analysis tool with three distinct lists (DHT-, TNFα- and DHT+TNFα regulated genes). All upregulated (shades of red; Z-score > 2, *P*-value < 0.05) and downregulated (shades of green, Z-score < −2, *P*-value < 0.05) biological function pathways are shown in the right side panel and a blowup of selected pathways in the left panel (full list in Supplementary Table S1). Biological functions that were uniquely upregulated in D+T are in red and those most activated in D+T treatment are in orange.

is however the exposure of a large group of latent NF-κB chromatin-binding sites. These results thus indicate that steroid receptors and NF-κB do not generally simply interfere with each other's transcriptional activity via direct physical interactions, as suggested based on previous gene-specific studies, but steroid receptors and NF-κB collaborate in receptor type- and, most likely, cell-specific ways to alter the repertoire of their chromatin-binding sites and modulate their target genes.

In conclusion, concomitant androgen and pro-inflammatory signaling can significantly reprogram AR and NF-κB cistromes. Androgen, in particular, is able to expose latent NF-κB-binding sites in the chromatin of PC cells, whereas TNFα can confine the AR cistrome. The mutual modulation of the cistromes and the enhancer activity involves FOXA1 and PIAS1 and PIAS2 proteins, resulting in the induction of a distinct transcription program which may contribute to the progression of PC.

SUPPLEMENTARY DATA

Supplementary Data are available at NAR Online.

ACKNOWLEDGEMENTS

The authors thank Merja Räsänen and Eija Korhonen for their assistance with cell culture. The EMBL GeneCore sequencing team is also acknowledged for deep sequencing and the UEF Bioinformatics Center for the help with data handling.

FUNDING

Finnish Cancer Organisations; Academy of Finland; Sigrid Jusélius Foundation. Funding for open access charge: Finnish Cancer Organisations; Academy of Finland.
Conflict of interest statement. None declared.

REFERENCES

1. Knudsen,K.E. and Scher,H.I. (2009) Starving the addiction: New opportunities for durable suppression of AR signaling in prostate cancer. *Clin. Cancer Res.*, **15**, 4792–4798.
2. Vis,A.N. and Schroder,F.H. (2009) Key targets of hormonal treatment of prostate cancer. part 2: the androgen receptor and 5alpha-reductase. *BJU Int.*, **104**, 1191–1197.

3. Shafi,A.A., Yen,A.E. and Weigel,N.L. (2013) Androgen receptors in hormone-dependent and castration-resistant prostate cancer. *Pharmacol. Ther.*, **140**, 223–238.
4. Oeckinghaus,A. and Ghosh,S. (2009) The NF-kappaB family of transcription factors and its regulation. *Cold Spring Harb. Perspect. Biol.*, **1**, a000034.
5. Mizokami,A., Gotoh,A., Yamada,H., Keller,E.T. and Matsumoto,T. (2000) Tumor necrosis factor-alpha represses androgen sensitivity in the LNCaP prostate cancer cell line. *J. Urol.*, **164**, 800–805.
6. Rodriguez-Berriguete,G., Sanchez-Espiridion,B., Cansino,J.R., Olmedilla,G., Martinez-Onsurbe,P., Sanchez-Chapado,M., Paniagua,R., Fraile,B. and Royuela,M. (2013) Clinical significance of both tumor and stromal expression of components of the IL-1 and TNF-alpha signaling pathways in prostate cancer. *Cytokine*, **64**, 555–563.
7. Karin,M. (2009) NF-kappaB as a critical link between inflammation and cancer. *Cold Spring Harb. Perspect. Biol.*, **1**, a000141.
8. Pahl,H.L. (1999) Activators and target genes of rel/NF-kappaB transcription factors. *Oncogene*, **18**, 6853–6866.
9. Ammirante,M., Luo,J.L., Grivennikov,S., Nedospasov,S. and Karin,M. (2010) B-cell-derived lymphotoxin promotes castration-resistant prostate cancer. *Nature*, **464**, 302–305.
10. Chmelar,R., Buchanan,G., Need,E.F., Tilley,W. and Greenberg,N.M. (2007) Androgen receptor coregulators and their involvement in the development and progression of prostate cancer. *Int. J. Cancer*, **120**, 719–733.
11. Rosenfeld,M.G., Lunyak,V.V. and Glass,C.K. (2006) Sensors and signals: a coactivator/corepressor/epigenetic code for integrating signal-dependent programs of transcriptional response. *Genes Dev.*, **20**, 1405–1428.
12. Malinen,M., Toropainen,S., Jääskeläinen,T., Sahu,B., Jänne,O.A. and Palvimo,J.J. (2015) Androgen receptor- and PIAS1-regulated gene programs in molecular apocrine breast cancer cells. *Mol. Cell. Endocrinol.*, **414**, 91–98.
13. Moilanen,A.M., Karvonen,U., Poukka,H., Yan,W., Toppari,J., Jänne,O.A. and Palvimo,J.J. (1999) A testis-specific androgen receptor coregulator that belongs to a novel family of nuclear proteins. *J. Biol. Chem.*, **274**, 3700–3704.
14. Rytinki,M.M., Kaikkonen,S., Pehkonen,P., Jääskeläinen,T. and Palvimo,J.J. (2009) PIAS proteins: Pleiotropic interactors associated with SUMO. *Cell Mol. Life Sci.*, **66**, 3029–3041.
15. Toropainen,S., Malinen,M., Kaikkonen,S., Rytinki,M., Jääskeläinen,T., Sahu,B., Jänne,O.A. and Palvimo,J.J. (2015) SUMO ligase PIAS1 functions as a target gene selective androgen receptor coregulator on prostate cancer cell chromatin. *Nucleic Acids Res.*, **43**, 848–861.
16. Hoefer,J., Schafer,G., Klocker,H., Erb,H.H., Mills,I.G., Hengst,L., Puhr,M. and Culig,Z. (2012) PIAS1 is increased in human prostate cancer and enhances proliferation through inhibition of p21. *Am. J. Pathol.*, **180**, 2097–2107.
17. Puhr,M., Hoefer,J., Eigentler,A., Dietrich,D., van Leenders,G., Uhl,B., Hoogland,M., Handle,F., Schlick,B., Neuwirt,H. *et al.* (2016) PIAS1 is a determinant of poor survival and acts as a positive feedback regulator of AR signaling through enhanced AR stabilization in prostate cancer. *Oncogene*, **35**, 2322–2332.
18. Liu,B., Yang,Y., Chernishof,V., Loo,R.R., Jang,H., Tahk,S., Yang,R., Mink,S., Shultz,D., Bellone,C.J. *et al.* (2007) Proinflammatory stimuli induce IKKalpha-mediated phosphorylation of PIAS1 to restrict inflammation and immunity. *Cell*, **129**, 903–914.
19. Liu,B., Yang,R., Wong,K.A., Getman,C., Stein,N., Teitell,M.A., Cheng,G., Wu,H. and Shuai,K. (2005) Negative regulation of NF-kappaB signaling by PIAS1. *Mol. Cell. Biol.*, **25**, 1113–1123.
20. Sahu,B., Pihlajamaa,P., Dubois,V., Kerkhofs,S., Claessens,F. and Jänne,O.A. (2014) Androgen receptor uses relaxed response element stringency for selective chromatin binding and transcriptional regulation in vivo. *Nucleic Acids Res.*, **42**, 4230–4240.
21. Gao,N., Zhang,J., Rao,M.A., Case,T.C., Mirosevich,J., Wang,Y., Jin,R., Gupta,A., Rennie,P.S. and Matusik,R.J. (2003) The role of hepatocyte nuclear factor-3 alpha (forkhead box A1) and androgen receptor in transcriptional regulation of prostatic genes. *Mol. Endocrinol.*, **17**, 1484–1507.
22. Jozwik,K.M. and Carroll,J.S. (2012) Pioneer factors in hormone-dependent cancers. *Nat. Rev. Cancer*, **12**, 381–385.
23. Sahu,B., Laakso,M., Ovaska,K., Mirtti,T., Lundin,J., Rannikko,A., Sankila,A., Turunen,J.P., Lundin,M., Konsti,J. *et al.* (2011) Dual role of FoxA1 in androgen receptor binding to chromatin, androgen signalling and prostate cancer. *EMBO J.*, **30**, 3962–3976.
24. Karvonen,U., Kallio,P.J., Jänne,O.A. and Palvimo,J.J. (1997) Interaction of androgen receptors with androgen response element in intact cells. roles of amino- and carboxyl-terminal regions and the ligand. *J. Biol. Chem.*, **272**, 15973–15979.
25. Rytinki,M.M., Kaikkonen,S., Sutinen,P. and Palvimo,J.J. (2011) Analysis of androgen receptor SUMOylation. *Methods Mol. Biol.*, **776**, 183–197.
26. Niskanen,E.A., Malinen,M., Sutinen,P., Toropainen,S., Paakinaho,V., Vihervaara,A., Joutsen,J., Kaikkonen,M.U., Sistonen,L. and Palvimo,J.J. (2015) Global SUMOylation on active chromatin is an acute heat stress response restricting transcription. *Genome Biol.*, **16**, 153.
27. Paakinaho,V., Kaikkonen,S., Makkonen,H., Benes,V. and Palvimo,J.J. (2014) SUMOylation regulates the chromatin occupancy and anti-proliferative gene programs of glucocorticoid receptor. *Nucleic Acids Res.*, **42**, 1575–1592.
28. Takayama,K., Suzuki,T., Tsutsumi,S., Fujimura,T., Urano,T., Takahashi,S., Homma,Y., Aburatani,H. and Inoue,S. (2014) RUNX1, an androgen- and EZH2-regulated gene, has differential roles in AR-dependent and -independent prostate cancer. *Oncotarget*, **6**, 2263–2276.
29. Sutinen,P., Malinen,M., Heikkinen,S. and Palvimo,J.J. (2014) SUMOylation modulates the transcriptional activity of androgen receptor in a target gene and pathway selective manner. *Nucleic Acids Res.*, **42**, 8310–8319.
30. Heinz,S., Benner,C., Spann,N., Bertolino,E., Lin,Y.C., Laslo,P., Cheng,J.X., Murre,C., Singh,H. and Glass,C.K. (2010) Simple combinations of lineage-determining transcription factors prime cis-regulatory elements required for macrophage and B cell identities. *Mol. Cell*, **38**, 576–589.
31. Schindelin,J., Arganda-Carreras,I., Frise,E., Kaynig,V., Longair,M., Pietzsch,T., Preibisch,S., Rueden,C., Saalfeld,S., Schmid,B. *et al.* (2012) Fiji: An open-source platform for biological-image analysis. *Nat. Methods*, **9**, 676–682.
32. Kaikkonen,M.U., Niskanen,H., Romanoski,C.E., Kansanen,E., Kivelä,A.M., Laitalainen,J., Heinz,S., Benner,C., Glass,C.K. and Ylä-Herttuala,S. (2014) Control of VEGF-A transcriptional programs by pausing and genomic compartmentalization. *Nucleic Acids Res.*, **42**, 12570–12584.
33. Ingolia,N.T., Ghaemmaghami,S., Newman,J.R. and Weissman,J.S. (2009) Genome-wide analysis in vivo of translation with nucleotide resolution using ribosome profiling. *Science*, **324**, 218–223.
34. Robinson,M.D., McCarthy,D.J. and Smyth,G.K. (2010) edgeR: A bioconductor package for differential expression analysis of digital gene expression data. *Bioinformatics*, **26**, 139–140.
35. Mizokami,A., Gotoh,A., Yamada,H., Keller,E.T. and Matsumoto,T. (2000) Tumor necrosis factor-alpha represses androgen sensitivity in the LNCaP prostate cancer cell line. *J. Urol.*, **164**, 800–805.
36. Orom,U.A. and Shiekhattar,R. (2013) Long noncoding RNAs usher in a new era in the biology of enhancers. *Cell*, **154**, 1190–1193.
37. Hah,N., Murakami,S., Nagari,A., Danko,C.G. and Kraus,W.L. (2013) Enhancer transcripts mark active estrogen receptor binding sites. *Genome Res.*, **23**, 1210–1223.
38. Nguyen,D.P., Li,J., Yadav,S.S. and Tewari,A.K. (2014) Recent insights into NF-kappaB signalling pathways and the link between inflammation and prostate cancer. *BJU Int.*, **114**, 168–176.
39. Strasner,A. and Karin,M. (2015) Immune infiltration and prostate cancer. *Front. Oncol.*, **5**, 128.
40. Ko,S., Shi,L., Kim,S., Song,C.S. and Chatterjee,B. (2008) Interplay of nuclear factor-kappaB and B-myb in the negative regulation of androgen receptor expression by tumor necrosis factor alpha. *Mol. Endocrinol.*, **22**, 273–286.
41. Nelius,T., Filleur,S., Yemelyanov,A., Budunova,I., Shroff,E., Mirochnik,Y., Aurora,A., Veliceasa,D., Xiao,W., Wang,Z. *et al.* (2007) Androgen receptor targets NFkappaB and TSP1 to suppress prostate tumor growth in vivo. *Int. J. Cancer*, **121**, 999–1008.
42. Palvimo,J.J., Reinikainen,P., Ikonen,T., Kallio,P.J., Moilanen,A. and Jänne,O.A. (1996) Mutual transcriptional interference between RelA and androgen receptor. *J. Biol. Chem.*, **271**, 24151–24156.

43. Aarnisalo,P., Palvimo,J.J. and Jänne,O.A. (1998) CREB-binding protein in androgen receptor-mediated signaling. *Proc. Natl. Acad. Sci. U.S.A.*, **95**, 2122–2127.
44. Drouin,J. (2014) Minireview: pioneer transcription factors in cell fate specification. *Mol. Endocrinol.*, **28**, 989–998.
45. Swinstead,E.E., Miranda,T.B., Paakinaho,V., Baek,S., Goldstein,I., Hawkins,M., Karpova,T.S., Ball,D., Mazza,D., Lavis,L.D. *et al.* (2016) Steroid receptors reprogram FoxA1 occupancy through dynamic chromatin transitions. *Cell*, **165**, 593–605.
46. Sahu,B., Laakso,M., Pihlajamaa,P., Ovaska,K., Sinielnikov,I., Hautaniemi,S. and Jänne,O.A. (2013) FoxA1 specifies unique androgen and glucocorticoid receptor binding events in prostate cancer cells. *Cancer Res.*, **73**, 1570–1580.
47. Wang,D., Garcia-Bassets,I., Benner,C., Li,W., Su,X., Zhou,Y., Qiu,J., Liu,W., Kaikkonen,M.U., Ohgi,K.A. *et al.* (2011) Reprogramming transcription by distinct classes of enhancers functionally defined by eRNA. *Nature*, **474**, 390–394.
48. Sutinen,P., Rahkama,V., Rytinki,M. and Palvimo,J.J. (2014) Nuclear mobility and activity of FOXA1 with androgen receptor are regulated by SUMOylation. *Mol. Endocrinol.*, **28**, 1719–1728.
49. Jin,R., Sterling,J.A., Edwards,J.R., DeGraff,D.J., Lee,C., Park,S.I. and Matusik,R.J. (2013) Activation of NF-kappa B signaling promotes growth of prostate cancer cells in bone. *PLoS One*, **8**, e60983.
50. Mabilleau,G. and Sabokbar,A. (2009) Interleukin-32 promotes osteoclast differentiation but not osteoclast activation. *PLoS One*, **4**, e4173.
51. Rao,N.A., McCalman,M.T., Moulos,P., Francoijs,K.J., Chatziioannou,A., Kolisis,F.N., Alexis,M.N., Mitsiou,D.J. and Stunnenberg,H.G. (2011) Coactivation of GR and NFKB alters the repertoire of their binding sites and target genes. *Genome Res.*, **21**, 1404–1416.
52. Schmidt,S.F., Larsen,B.D., Loft,A., Nielsen,R., Madsen,J.G. and Mandrup,S. (2015) Acute TNF-induced repression of cell identity genes is mediated by NFkappaB-directed redistribution of cofactors from super-enhancers. *Genome Res.*, **25**, 1281–1294.
53. Franco,H.L., Nagari,A. and Kraus,W.L. (2015) TNFalpha signaling exposes latent estrogen receptor binding sites to alter the breast cancer cell transcriptome. *Mol. Cell*, **58**, 21–34.